Collisional Quenching of the $2S$ State of Muonic Hydrogen

T.S. JENSEN[a,b] AND V.E. MARKUSHIN[a]

[a] *Paul Scherrer Institut, CH-5232 Villigen PSI, Switzerland*

[b] *Institut für Theoretische Physik der Universität Zürich, Winterthurerstrasse 190, CH-8057 Zürich, Switzerland*

Abstract

We have calculated differential, total and transport cross sections for muonic hydrogen in the $n = 2$ state scattering from hydrogen. The metastable fraction of the $2S$ state that slows down below the $2P$ threshold without undergoing collisional quenching has been calculated as a function of the initial kinetic energy using a Monte Carlo kinetics program. Contrary to earlier estimates, the metastable fraction in the kinetic energy range of $2 - 5$ eV cannot be neglected.

arXiv:nucl-th/0001009v1 5 Jan 2000

1 Introduction

The $2S$ state of muonic hydrogen offers interesting possibilities to do precision tests of QED and to determine the proton RMS charge radius (see [1] and references therein). An isolated $(\mu p)_{2S}$ is metastable with a lifetime mainly determined by muon decay (about 2.2 μs). In liquid or gaseous hydrogen the lifetime of the $2S$ state is shortened considerably because of Stark mixing followed by $2P \rightarrow 1S$ radiative transitions. If a sizeable fraction of muonic hydrogen atoms ends up in the $2S$ state with a sufficiently long lifetime, then precision laser experiments with this metastable $2S$ state become feasible. If the $(\mu p)_{2S}$ has kinetic energy below the $2P$ threshold (laboratory kinetic energy $T_0 = 0.3$ eV), then Stark transitions $2S \rightarrow 2P$ are energetically forbidden[1]. The metastable fraction of $(\mu p)_{2S}$ in hydrogen depends on the kinetic energy at the time of formation.

The first estimate of the $(\mu p)_{2S}$ lifetime was done by Kodosky and Leon [5]. They calculated the inelastic $2S \rightarrow 2P$ cross section in a semiclassical framework and concluded that the $2S$ state for $T > T_0$ will be rapidly depopulated except for very small target densities. However, this model did not consider deceleration due to elastic $2S \rightarrow 2S$ scattering. A more elaborate approach was developed by Carboni and Fiorentini [6]. They calculated both elastic $2S \rightarrow 2S$ and inelastic $2S \rightarrow 2P$ cross sections quantum mechanically and estimated the probability for a $(\mu p)_{2S}$ atom to slow down below threshold from a given initial energy. The results of their calculations show that a sizeable fraction of $(\mu p)_{2S}$ formed at kinetic energies less than 1.3 eV can slow down below the $2P$ threshold.

The metastable fraction of $(\mu p)_{2S}$ per stopped muon can in principle be calculated in a cascade model which takes the different processes (Stark mixing, radiative decays, etc.) into account [7,8]. However, if one knows the fraction of stopped muons which reaches the $2S$ state (regardless of energy) and the kinetic energy distribution on arrival in this state, then it is sufficient to treat the final part of the cascade ($n = 1, 2$). This information can be obtained from experiments. The fraction of stopped muons which arrives in the $2S$ state can be determined from the radiative yields [9–11]: it was found in Ref. [9] that between 2% and 7% of the μp reach the $2S$ state in the pressure range $0.33 - 800$ hPa. The kinetic energy distribution for μp in the $1S$ state, which for low pressures is expected to be very similar to that of the $2S$ state just after arrival, can be obtained from diffusion experiments [12, 13]. The median energy is found to be about 1.5 eV for a

---

[1] Some quenching will, however, occur because $2S - 2P$ mixing during collisions allows radiative transitions to the $1S$ state (See Refs. [2–4]).
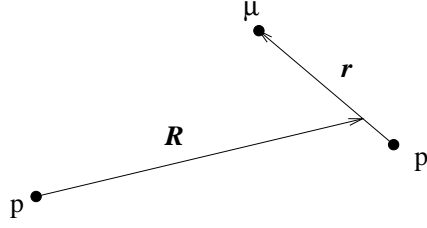
Figure 1: Coordinates used in the calculations: $\boldsymbol{R}$ is the vector from the target proton to the center of mass of the μp, $\boldsymbol{r}$ is the relative vector of the μp system.

target pressure of 0.25 hPa [13].

The purpose of this paper is to calculate the fraction of μp in the $2S$ state which reaches kinetic energies below the $2P$ threshold as a function of the initial kinetic energy T. We will also present a fully quantum mechanical calculation of μp+H differential cross sections which are used in our Monte Carlo simulation of the kinetics.

The paper is organized as follows. The theoretical framework of the quantum mechanical calculation of the cross sections is outlined in Section 2. The calculated cross sections are discussed in Section 3. Section 4 presents the calculations of the metastable $2S$ fraction. The summary of the results is given in Section 5.

Unless otherwise stated, atomic units ($\hbar = a_0 = m_e = 1$) are used throughout this paper. The unit of cross section is $a_0^2 = 2.8 \cdot 10^{-17} \text{cm}^2$.

2 Quantum Mechanical Approach to the Calculation of the Cross Sections $(\mu p)_{nl} + \text{H} \rightarrow (\mu p)_{nl'} + \text{H}$

For the benefit of the reader, we briefly describe the quantum mechanical calculation of μp+H scattering in the coupled-channel approximation. The three-body wave function $\psi(\boldsymbol{r}, \boldsymbol{R})$ where the coordinates $\boldsymbol{r}$ and $\boldsymbol{R}$ are defined in Fig. 1 satisfies the Schrödinger equation

$$H\psi(\boldsymbol{r}, \boldsymbol{R}) = E\psi(\boldsymbol{r}, \boldsymbol{R}) \tag{1}$$

3

where the Hamiltonian is given by

$$H = -\frac{\nabla^2}{2\mu} + H_{\mu p} + V(\boldsymbol{r}, \boldsymbol{R}) \quad . \tag{2}$$

Here $\mu = m_p m_{\mu p}/(m_p + m_{\mu p})$ is the reduced mass of the $p - \mu p$ system, with m_p being the proton mass and $m_{\mu p}$ the total μp mass. The two-body Hamiltonian of the μp atom, $H_{\mu p}$, includes the Coulomb interaction and a term that describes the shift of the nS state (mainly because of the vacuum polarization) with respect to the states with $l > 0$. For the case $n = 2$ considered below, the $2S$ state is lower than the $2P$ by $\Delta E = 0.21$ eV. The much smaller fine and hyperfine structure splitting is neglected. The potential $V(\boldsymbol{r}, \boldsymbol{R})$ describes the interaction of the μp system with the target proton[2]:

$$V(\boldsymbol{r}, \boldsymbol{R}) = \frac{1}{|\boldsymbol{R} - \epsilon \boldsymbol{r}|} - \frac{1}{|\boldsymbol{R} + (1 - \epsilon)\boldsymbol{r}|} \tag{3}$$

where $\epsilon = m_\mu/m_{\mu p} = 0.101$.

Equation (1) is solved in the coupled-channel approximation by using a finite number of basis functions to describe the state of the μp. For the problem of $nlm \to nl'm'$ scattering considered in this paper, the set of n^2 eigenstates with principal quantum number n has been selected but the basis can be extended in a straightforward manner. With n fixed, let $\chi_{lm}(\boldsymbol{r})$ denote the normalized eigenfunctions of the atomic Hamiltonian $H_{\mu p}$ with the energy E_{nl}, the square of the μp internal angular momentum $\mathbf{l}^2$ (eigenvalue $l(l+1)$) and its projection along the z-axis l_z (eigenvalue m). The total wave function $\psi(\boldsymbol{r}, \boldsymbol{R})$ is expanded as follows

$$\psi(\boldsymbol{r}, \boldsymbol{R}) = R^{-1} \sum_{JMLl} \xi_{JLl}(R) \mathcal{Y}_{Ll}^{JM}(\boldsymbol{\Omega}, \boldsymbol{r}) \tag{4}$$

where

$$\mathcal{Y}_{Ll}^{JM}(\boldsymbol{\Omega}, \boldsymbol{r}) = \sum_{M_L m} \langle LlM_L m | JM \rangle Y_{LM_L}(\boldsymbol{\Omega}) \chi_{lm}(\boldsymbol{r}), \quad \boldsymbol{\Omega} = \boldsymbol{R}/R \quad . \tag{5}$$

are simultaneous eigenfunctions of $\mathbf{J}^2$, $\mathbf{L}^2$, $\mathbf{l}^2$ and J_z with eigenvalues $J(J+1)$, $L(L+1)$, $l(l+1)$ and M, respectively. Here $\mathbf{L}$ is the $p - \mu p$ relative angular momentum, $\mathbf{J} = \mathbf{L} + \mathbf{l}$ is the total orbital angular momentum of the system.

---

[2]For the sake of simplicity, we ignore the fact that the protons are identical particles.

For a given value of J the system of radial Schrödinger equations has the form

$$\left(-\frac{1}{2\mu}\frac{d^2}{dR^2}+\frac{L(L+1)}{2\mu R^2}+E_{nl}-E\right)\xi_{JLl}(R)+\sum_{L'l'}\langle L'l'JM|V|LlJM\rangle\xi_{JL'l'}(R) = 0 \tag{6}$$

where the potential matrix elements are calculated in the basis (5):

$$\langle\boldsymbol{\Omega},\boldsymbol{r}|LlJM\rangle = \mathcal{Y}_{Ll}^{JM}(\boldsymbol{\Omega},\boldsymbol{r}) \quad . \tag{7}$$

The matrix elements of the potential (3) have been calculated analytically; the corresponding formulas are rather lengthy and will be given elsewhere. From the asymptotic form of the solution of the n^2 coupled[3] equations (6), the scattering matrix S is extracted and cross sections can be calculated using standard formulas. The scattering amplitude for $nlm \to nl'm'$ is given by

$$f_{nlm\to nl'm'}(\boldsymbol{\Omega}) = \frac{4\pi}{2i\sqrt{k'k}}\sum_{L'LM'_L}i^{L-L'}Y_{L'M'_L}(\boldsymbol{\Omega})\langle L'l'M'_Lm'|S-1|Ll0m\rangle Y^*_{L0}(0) \tag{8}$$

where

$$\langle L'l'M'_Lm'|S|Ll0m\rangle = \sum_{JM}\langle L'l'M'_Lm'|JM\rangle\langle JM|Ll0m\rangle\langle L'l'J|S|LlJ\rangle \quad . \tag{9}$$

As a consequence of rotational symmetry, the matrix elements $\langle L'l'J|S|LlJ\rangle$ do not depend on the quantum number M. The differential cross sections for the transitions $nl \to nl'$ are given by

$$\frac{d\sigma_{nl\to nl'}}{d\Omega} = \frac{1}{(2l+1)}\sum_{m'm}\frac{k'}{k}|f_{nlm\to nl'm'}|^2 \tag{10}$$

where k and k' are the magnitudes of the relative momenta in the initial and final state, correspondingly.

The total cross sections of the transitions $nl \to nl'$ have the form

$$\sigma_{nl\to nl'} = \frac{1}{(2l+1)}\frac{\pi}{k^2}\sum_J(2J+1)\sum_{LL'}|\langle L'l'J|S-1|LlJ\rangle|^2 \tag{11}$$

---

[3] Because of parity conservation the equations decouple into two sets of respectively $n(n+1)/2$ and $n(n-1)/2$ coupled equations.

and the corresponding transport cross sections are given by

$$\sigma_{nl \to nl'}^{tr} = \int d\Omega (1 - \cos\theta) \frac{d\sigma_{nl \to nl'}}{d\Omega} \quad . \tag{12}$$

In order to treat the long distance behaviour of the μp+H interaction properly, the effect of electron screening must be taken into account. This is done by multiplying the matrix elements $\langle L'l'JM|V|LlJM\rangle$ in Eq. (6) by the screening factor

$$F(R) = (1 + 2R + 2R^2)e^{-2R} \tag{13}$$

which corresponds to the assumption that the electron of the hydrogen atom remains unaffected in the $1S$ state during the collision.

For $p - \mu p$ separations R smaller than a few units of the μp Bohr radius, $a_\mu = 0.0054$, our model cannot be expected to be valid because the truncated set of basis functions in Eq. (4) is not sufficient to describe the total three-body wave function $\psi(\boldsymbol{r}, \boldsymbol{R})$. Furthermore, exchange symmetry between the two protons must be taken into account. We can estimate the sensitivity of our results to the short range part of the interaction by using the dipole approximation for the potential (3). The interaction in the dipole approximation is given by the first nonzero term in the expansion of Eq. (3) in inverse powers of R:

$$V_{DA}(\boldsymbol{r}, \boldsymbol{R}) = \frac{\boldsymbol{r} \cdot \boldsymbol{R}}{R^3} = \frac{z}{R^2} \quad . \tag{14}$$

A certain problem arises in the dipole approximation for a few low partial waves ($J \leq 5$): the Schrödinger equation becomes ill defined because of the attractive $1/R^2$ singularity[4]. Following Ref. [6] we cure this difficulty by placing an infinitely repulsive sphere of radius $r_{\min}$ around the target proton. The sensitivity of the results to this cutoff parameter $r_{\min}$ will be used below as an estimate of the importance of detailed description of the interaction at short distances.

In this paper we are interested in the $2l \to 2l'$ transitions, and only four states $n = 2$ are used to describe the μp part of the total wave function. The four coupled second order equations (6) are solved numerically for $J = 0, 1, ..., J_{\max}$ where the highest partial wave $J_{\max}$ is chosen large enough to ensure the convergence of the partial wave expansion at given collision energy.

---

[4]This is a problem only in the dipole approximation. The exact matrix elements are all finite for $R = 0$.

Until now we have considered the μp collisions with the atomic target. Treating the collisions with hydrogen molecules is a formidable task (even for μp in the ground state [14]) which we do not attempt here. The inelastic threshold T_0 for $2S \rightarrow 2P$ transitions is 0.44 eV for atomic target and 0.33 eV for a molecular target. To get the correct threshold value for the inelastic cross sections one can substitute the atomic hydrogen mass with the molecular one. By varying $r_{\min}$ and the target mass one can obtain an estimate of the theoretical uncertainty of our approach.

The present model for calculating cross sections for $(\mu p)_{n=2} - \text{H}$ scattering is a straightforward extension of the one by Carboni and Fiorentini [6]. There are three major differences: we solve the four coupled differential equations exactly while Ref. [6] treated non adiabatic terms as a perturbation. The second difference is that we include the full angular coupling while Ref. [6] omitted some minor terms. Finally, we use exact matrix elements for the $\mu p - p$ interaction while Ref. [6] considers only the dipole approximation. These approximations were justified by Ref. [6] as follows: for small kinetic energies the velocity of the muonic hydrogen atom is so low that the motion can be regarded as nearly adiabatic. The angular coupling terms that were omitted in Ref. [6] are of the order 1 which is much smaller than the remaining angular coupling terms of the order of $J(J+1)$ (the angular momenta as high as $J \sim 15$ contribute to the $2S \rightarrow 2P$ cross section at $T = 1$ eV). The electric field from a hydrogen atom is strong enough to induce Stark transitions in the μp for the distances $R \sim a_0$. Therefore, the regions where the dipole approximation is valid ($R \gg a_\mu$) are supposed to be most important. The diffusion experiments [12,13] have shown that a sizeable fraction of $(\mu p)_{n=2}$ atoms has kinetic energies of several eV. In this high energy region the non adiabatic couplings become strong and the model of Ref. [6] can not be expected to give accurate results.

The problem of $\mu p + \text{H}$ scattering has been treated fully quantum mechanically in Refs. [16–19]. However, these calculations did not include the $2S - 2P$ energy splitting and the question of the metastability of $(\mu p)_{2S}$ was not addressed. Stark mixing has been studied in the semiclassical straight-line-trajectory approximation in Refs. [5, 15, 20]. We have calculated the $2S \rightarrow 2P$ Stark mixing cross sections in the semiclassical approach in order to compare with the quantum mechanical results. A more detailed comparison between semiclassical and quantum mechanical calculations of $\mu p + \text{H}$ scattering will be given elsewhere.
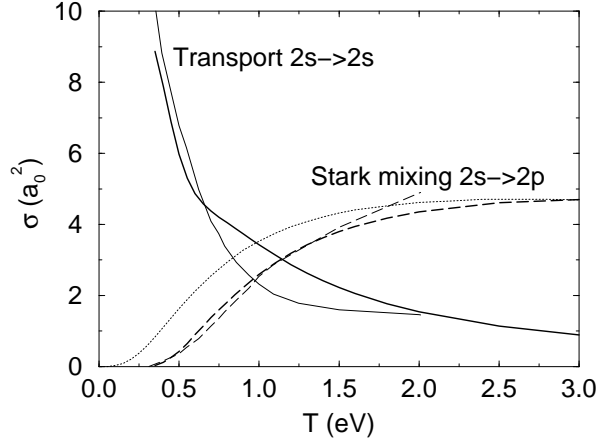
7

Figure 2: Transport cross section $2S \to 2S$ (solid lines) and Stark mixing cross section $2S \to 2P$ (long-dashed lines) vs. laboratory kinetic energy T. The thick lines are the results of the present calculations, the thin lines are obtained from Fig. 3 of Ref. [6] and the dotted line shows the result of the semiclassical calculation in the straight-line-trajectory approximation. The quantum mechanical cross sections are calculated with $M_{\text{target}} = M_{\text{H}_2}$.

3   The Cross Sections of $(\mu p)_{2l}$ Scattering from Hydrogen

Using the method described in Section 2 the S-matrix has been calculated for the laboratory kinetic energy range $T_0 < T < 6$ eV. Unless otherwise explicitly stated, the results shown are obtained with the exact potential (3). Electron screening is always taken into account. Both atomic and molecular mass of the target ($M_{\text{target}} = M_{\text{H}}$, M_{H_2}) have been used.

Figure 2 shows the $2S \to 2S$ transport cross section and the $2S \to 2P$ Stark mixing cross section in comparison with the results from Ref. [6] (the molecular mass is used in both cases). There is a good agreement for the Stark mixing $2S \to 2P$ cross section below 1.7 eV. For the $2S \to 2S$ transport cross section, the agreement is fair, with the discrepancy being typically less than 30%.

In order to estimate the theoretical uncertainty of our approach, we calculated the cross sections in the dipole approximation with short distance cutoff $0.01 \le r_{\min} \le 0.05$ for $M_{\text{target}} = M_{\text{H}}$ and $M_{\text{target}} = M_{\text{H}_2}$. For fixed value of M_{target}, the cross sections for the three reactions $2S \to 2P$, $2P \to 2S$ and $2P \to 2P$ are weakly dependent on $r_{\min}$. This shows that these reactions
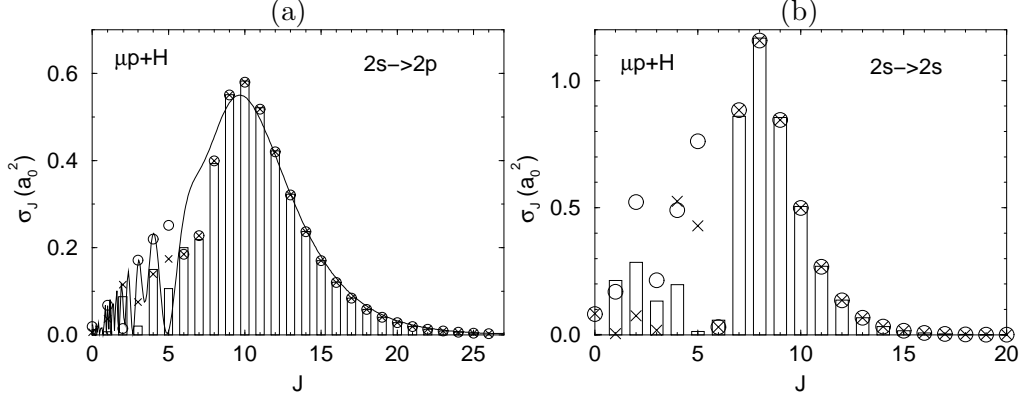
8

Figure 3: Partial wave cross sections for the reactions $2S \rightarrow 2P$ (a) and $2S \rightarrow 2S$ (b) at laboratory kinetic energy 3 eV and $M_{\text{target}} = M_{\text{H}}$. The histograms show the results for exact matrix elements; the dipole approximation with $r_{\min} = 0.01$ and $r_{\min} = 0.05$ is shown by o and $\times$, respectively. The semiclassical result for the $2S \rightarrow 2P$ transition is shown with a solid line.

are dominated by the long range part of the interaction $V(\boldsymbol{r}, \boldsymbol{R})$. The only process rather sensitive to the value of $r_{\min}$ is the elastic scattering $2S \rightarrow 2S$. This can be understood by considering the adiabatic energy curves for low angular momentum. The energy curve which corresponds asymptotically to the $2S$ state is attractive while those corresponding to the three $2P$ states are repulsive. Therefore, in the adiabatic approximation the $2S \rightarrow 2S$ cross sections are expected to depend on the short range part of the potential while this is not the case for $2P \rightarrow 2P$ scattering. At energies above 2 eV the semiclassical approximation is in a good agreement with our quantum mechanical results. However, this semiclassical approximation does not treat the threshold behaviour correctly.

A more detailed comparison of the approximations used can be done by plotting the J dependence of the partial wave cross sections σ_J at fixed energy as shown in Fig. 3. The quantum mechanical results obtained for the exact potential and the dipole approximation with the short range cutoff agree well for angular momentum $J > 5$ while the lowest partial waves are sensitive to the short range behaviour of the approximating potentials. The reason is that for $J > 5$ the centrifugal barrier is strong enough to prevent the μp from approaching close to the target proton. For $J \leq 5$ the μp can get very close to the proton and the use of a small number of atomic orbitals is not sufficient — a better description in this region is needed in a true three–
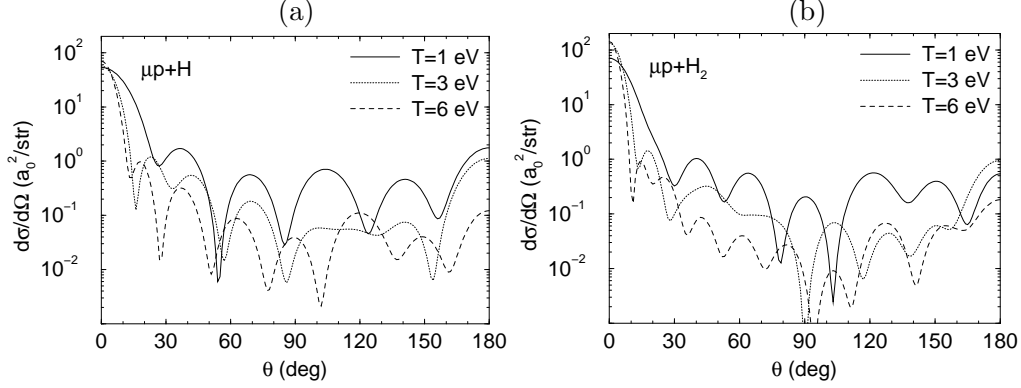
9

Figure 4: Differential $2S \to 2S$ cross sections vs. CMS scattering angle θ for three different laboratory kinetic energies: (a) $M_{\text{target}} = M_{\text{H}}$, (b) $M_{\text{target}} = M_{\text{H}_2}$.

body framework. It is seen that a substantial part of the $2S \to 2S$ cross section comes from partial waves with low J, so this result also explains why the uncertainty of the elastic $2S$ cross section is larger than for the other reactions. The semiclassical calculation can be compared with the partial wave cross sections by using the relation between the impact parameter ρ, the relative momentum k and the angular momentum J

$$k\rho = J + 1/2 \quad . \tag{15}$$

For large J (large impact parameter) there is a very good agreement between the semiclassical contribution to the $2S \to 2P$ cross section and the quantum mechanical partial wave result. An example of the differential cross sections for the reaction $2S \to 2S$ given in Fig. 4 shows a characteristic pattern with a strong forward peak and a set of maxima and minima, which is in qualitative agreement with Ref. [18] where the adiabatic approach was used.

4 The Surviving Fraction of the Metastable $(\mu p)_{2S}$ State

The surviving metastable fraction $f(T)$ is defined as the probability that the μp atom in the $2S$ state with initial kinetic energy T reaches the energy below the $2P$ threshold by slowing down in elastic collisions. Assuming that the rate of the radiative transition $2P \to 1S$, $\lambda_{2P \to 1S} = 1.2 \cdot 10^{11}$ s^{-1}, is much
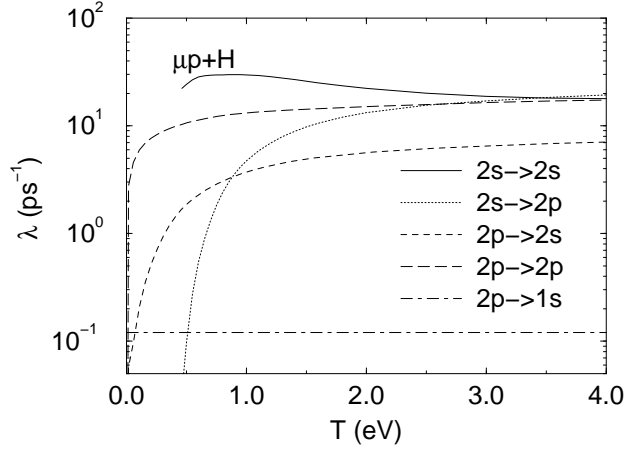
10

Figure 5: Collisional rates for $2l \rightarrow 2l'$ in liquid hydrogen ($N = N_0$, $M_{\text{target}} = M_{\text{H}}$) and the radiative $2P \rightarrow 1S$ transition rate.

larger than the Stark mixing rate[5], the surviving fraction $f(T)$ was estimated in [6] by the formula

$$f(T) = \exp\left(-\frac{(m_{\mu p} + M_{\text{target}})^2}{2m_{\mu p}M_{\text{target}}} \int_{T_0}^{T} \frac{\sigma_{2S \rightarrow 2P}(T')}{T'\sigma_{2S \rightarrow 2S}^{tr}(T')} dT'\right) \qquad (16)$$

with $M_{\text{target}} = M_{\text{H}_2}$. It was found that a sizeable fraction of $(\mu p)_{2S}$ atoms formed at kinetic energies below 1.3 eV slows down below threshold.

Equation (16) is based on the approximation of continuous energy loss. To provide a more realistic treatment of the evolution in kinetic energy we use a Monte Carlo program based on the differential cross sections for the four processes $2S \rightarrow 2S$, $2S \rightarrow 2P$, $2P \rightarrow 2S$ and $2P \rightarrow 2P$. In addition to the collisional processes, the $2P \rightarrow 1S$ radiative transition is also included in the code. The fate of a μp formed in the $2S$ state with kinetic energy T is thus either to undergo $2P \rightarrow 1S$ radiative transition after the Stark mixing $2S \rightarrow 2P$ or to end up in the $2S$ state with kinetic energy below the threshold with probability $f(T)$. Figure 5 shows the rates, $\lambda_{2l \rightarrow 2l'} = N_0 v \sigma_{2l \rightarrow 2l'}$, for the collisional transitions in liquid hydrogen in comparison with the radiative deexcitation rate $\lambda_{2P \rightarrow 1S}$. In liquid hydrogen the Stark mixing rates are so large that the μp states are expected to be statistically populated for kinetic energies $T \geq 2$ eV (where threshold effects can be neglected).

[5]With our result for the Stark mixing rate $2P \rightarrow 2S$ at 1 eV as a function of the target density N, $\lambda_{2P \rightarrow 2S} = N v \sigma_{2P \rightarrow 2S} \approx 4 \cdot 10^{12}(N/N_0)$ s^{-1} where N_0 is the liquid hydrogen density $4.25 \cdot 10^{22}$ atoms/cm^3, the range of validity is $N \ll 0.03N_0$.
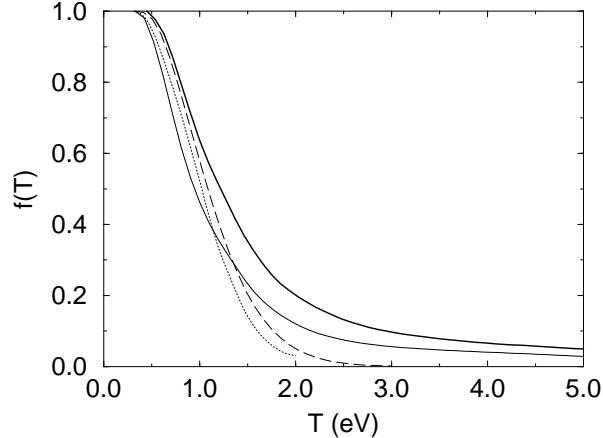
Figure 6: The metastable surviving fraction $f(T)$ of the $(\mu p)_{2S}$ states vs. initial kinetic energy T. The thick and thin solid lines show the results of Monte Carlo calculations with $M_{\text{target}} = M_{\text{H}}$ and $M_{\text{target}} = M_{\text{H}_2}$, respectively. The dotted line shows the result of Carboni and Fiorentini [6] and the long-dashed line shows $f(T)$ calculated using the method of Ref. [6] (Eq. (16)) with our cross sections. The results are valid for densities $N \leq 10^{-2} N_0$.

Figure 6 shows the surviving fraction $f(T)$ calculated with the Monte Carlo program for target density $10^{-6} < N/N_0 < 10^{-2}$. The approximation (16) gives somewhat higher values for the survival probability than the exact kinetics calculation at $T < 1.4$ eV. The Monte Carlo results at high energies ($T > 1.5$ eV) are significantly larger than those obtained from Eq. (16) where continuous energy loss is assumed. The reason is that the backward scattering (see Fig. 4) with maximum possible energy loss plays an important role in bringing the $(\mu p)_{2S}$ atoms below the $2P$ threshold for higher energies.

In order to estimate the theoretical uncertainty of $f(T)$ we performed the Monte Carlo calculation with the cross sections obtained in the dipole approximation. In all cases the Monte Carlo calculations are consistent with the results corresponding to the exact potential: at 2 eV the surviving fraction is in the range $15-20\%$ for atomic target mass and $10-16\%$ for molecular target mass. The use of the target mass M_{H} instead of M_{H_2} leads to somewhat higher survival fractions because of a simple kinematical reason: the loss of kinetic energy in a collision with the same angle in the CMS is larger for the target of smaller mass and, furthermore, the inelastic threshold is higher for the scattering from the atomic target. Merely substituting the atomic mass with the molecular mass for the hydrogen target does not account for the additional energy loss due to rotational and vibrational excitations of

12

H_2. One would therefore expect that the slowing down process is more efficient than this model suggests and the survival probability calculated with molecular target mass is underestimated. The opposite is true for calculations with atomic target: here the transfer of kinetic energy from the μp to the individual hydrogen atoms is not restricted by molecular bindings. Thus results with atomic target probably give somewhat optimistic results for the surviving fraction.

5   Conclusion

The main results of this paper can be summarized as follows. The detailed Monte Carlo kinetics calculations predict the surviving metastable fraction of the $2S$ state of μp to be larger than 50% for the initial kinetic energy 1 eV in agreement with earlier estimates [6]. For higher initial kinetic energies, our result is significantly larger than the earlier estimates: the surviving metastable fraction for $T = 5$ eV is about 4%. This effect is due to a sizeable contribution of backward scattering in elastic collisions.

Our Monte Carlo calculations are based on the cross sections calculated in the coupled-channel approximation. The main limitation of this method for the problem concerned comes from the use of a small number of atomic states to describe the μp system and the neglect of the molecular structure of the target. A more accurate treatment of the μpp three body problem is needed in order to do reliable calculations for a few lowest partial wave amplitudes. Our approach, however, is well suited for the description of the collisions with the characteristic scale of impact parameters of the order of a_0 which is exactly the case for the problem involved. Therefore our results provide a significantly improved basis for a better estimate of the metastable $(\mu p)_{2S}$ fraction [21] which is very important for the planned Lamb–shift experiment at PSI [1].

Further details and more results concerning the scattering of the μp atoms in the excited states $n \geq 2$ will be published elsewhere.

Acknowledgement

References

[1] D. Taqqu et al., Hyperfine Interactions **119**, 311 (1999)

[2] R.O. Mueller et al., Phys. Rev. **A11**, 1175 (1975)

[3] J.S. Cohen and J.N. Bardsley, Phys. Rev. **A23**, 46 (1981)

[4] L.I. Menshikov and L.I. Ponomarev, Z. Phys. **D2**, 1 (1986)

[5] G. Kodosky and M. Leon, Nuovo Cimento **1B**, 41 (1971)

[6] G. Carboni and G. Fiorentini, Nuovo Cimento **39B**, 281 (1977)

[7] V.E. Markushin, Phys. Rev. **A50**, 1137 (1994)

[8] V.E. Markushin, Hyperfine Interaction **119**, 11 (1999)

[9] H. Anderhub et al., Phys. Lett. **143B**, 65 (1984)

[10] M. Bregant et al., Phys. Lett. **241A**, 344 (1998)

[11] B. Lauss et al., Phys. Rev. Lett. **80**, 3041 (1998)

[12] F.J. Hartmann et al., Hyperfine Interactions **101/102**, 623 (1996)

[13] F. Kottmann et al., Hyperfine Interactions **119**, 3 (1999)

[14] A. Adamczak, Hyperfine Interactions **82**, 91 (1993)

[15] M. Leon and H.A. Bethe, Phys. Rev. **127**, 636 (1962)

[16] V.P. Popov and V.N. Pomerantsev, Hyperfine Interactions **101/102**, 133 (1996)

[17] V.P. Popov and V.N. Pomerantsev, Hyperfine Interactions **119**, 133 (1999)

[18] V.P. Popov and V.N. Pomerantsev, Hyperfine Interactions **119**, 137 (1999)

[19] V.V. Gusev, V.P. Popov and V.N. Pomerantsev, Hyperfine Interactions **119**, 141 (1999)

[20] T.P. Terada and R.S. Hayano, Phys. Rev. **C55**, 73 (1997)

[21] P. Hauser et al., to be published.